

CONTROL OF LASER RADIATION PARAMETERS

PACS numbers: 42.25.Kb; 42.55.Wd ; 42.81.Qb
DOI: 10.1070/QE2014v044n04ABEH015230

A high-speed, high-efficiency phase controller for coherent beam combining based on SPGD algorithm

Z.M. Huang, C.L. Liu, J.F. Li, D.Y. Zhang

Abstract. **A phase controller for coherent beam combining (CBC) of fibre lasers has been designed and manufactured based on a stochastic parallel gradient descent (SPGD) algorithm and a field programmable gate array (FPGA). The theoretical analysis shows that the iteration rate is higher than 1.9 MHz, and the average compensation bandwidth of CBC for 5 or 20 channels is 50 kHz or 12.5 kHz, respectively. The tests show that the phase controller ensures reliable phase locking of lasers: When the phases of five lasers are locked by the improved control strategy with a variable gain, the energy encircled in the target is increased by 23 times than that in the single output, the phase control accuracy is better than $\lambda/20$, and the combining efficiency is 92%.**

Keywords: *coherent optics, fibre laser arrays, beam combining, stochastic parallel gradient descent, phase controller.*

1. Introduction

High-power and good-beam-quality lasers have a wide range of applications in materials processing, medicine and sensors. Because of the restrictions due to thermal and nonlinear effects, radiation from a single laser cannot have an immense energy while maintaining a high beam quality. The successful recent demonstrations of high-power coherent beam combining (CBC) systems with active phase-locking of a master oscillator power amplifier (MOPA) array [1–9] show a way to achieve high brightness beyond the limit of a single laser source.

The key element of this technique is active phasing, which has been proposed in many approaches, e.g., heterodyne detection phase control technique [10], multi-dithering technique [11, 12], phase control technique of the stochastic parallel gradient descent (SPGD) algorithm [13, 14] and single-frequency dithering technique [15]. Coherent beam combining of n channels by the heterodyne method requires n photodetectors and n-channel signal processing circuits; as a result, such a system becomes too complicated. Although multi-dithering and single-frequency dithering methods require only a single detector, they still need modulation and demodulation for the n-channel signals, and the control strategies are complex. A CBC system based on the SPGD optimisation algorithm is simple and compact, which makes it widely used. The phase controller is the core of CBC systems based on the SPGD algorithm.

In 2005, Liu et al. [13] designed a computer-based SPGD phase controller. The iteration rate was 16 kHz and the control bandwidth was 310 Hz. In 2007, they had used an AVR microprocessor instead of the computer and the iteration rate of the controller increased up to 95 kHz, while the compensation control bandwidth reached 100 Hz [16]. In 2009, they improved the controller: The iteration rate of coherent combining for seven channels reached 1 kHz, and the phase noise control bandwidth was 1 kHz [17]. In 2009, Yang Ruo-fu obtained coherent combining of two fibre amplifiers using a DSP processor based on the SPGD algorithm at the control bandwidth of 50 Hz [18]. In 2010, Wang Xiao-lin [19] designed a phase controller based on the SPGD algorithm using a DSP processor for two channel coherent combining: The iteration rate was up to 200 kHz, and the average control bandwidth was greater than 12.5 kHz.

In addition, the researchers designed controllers based on the SPGD algorithm for the beam purification and adaptive optics applications. Wang San-hong et al. [20] controlled 37 units of the deformable mirror system utilising the beam purification controller based on the SPGD algorithm, while the iteration rate was about 100Hz. In this paper, a phase controller based on the SPGD algorithm for coherent beam combining was designed using a field programmable gate array (FPGA).

2. Principle of coherent combining based on the SPGD algorithm

The MOPA configuration for SPGD-based coherent combining is shown in Fig. 1. The laser beam passing through an optical isolator is split into five beams, which are controlled by five $LiNbO_3$ phase modulators. The five fibre outputs are combined via an integrated beam combiner, which can be replaced in a high power system by diffractive optical elements, for example. Then, the light passes through a fibre-coupled beam collimator (an output beam of 14 mm in diameter) and next is split by a 50 : 50 beam splitter. The transmitted beam goes through a lens with a focal length of 1 m into a CCD camera, and the reflected beam goes through a similar lens into a photodetector (the photodetector is an InGaAs amplifier with a 700- to 1800-nm response wavelength, 800-μm aperture size, and 17-MHz bandwidth at a gain of 0 dB) placed in the focal plane. The output signal from the photodetector after AD conversion is fed into the optimised algorithm controller.

Then, precise phase control is implemented by the phase modulator using the SPGD algorithm, consisting of an infi-

Z.M. Huang, C.L. Liu, J.F. Li, D.Y. Zhang Institute of Fluid Physics, China Academy of Engineering Physics, Sichuan, Mianyang 621900, China; e-mail: zhimenghuang@126.com

Received 16 May 2013; revision received 14 October 2013
Kvantovaya Elektronika **44** (4) 301–305 (2014)
Submitted in English

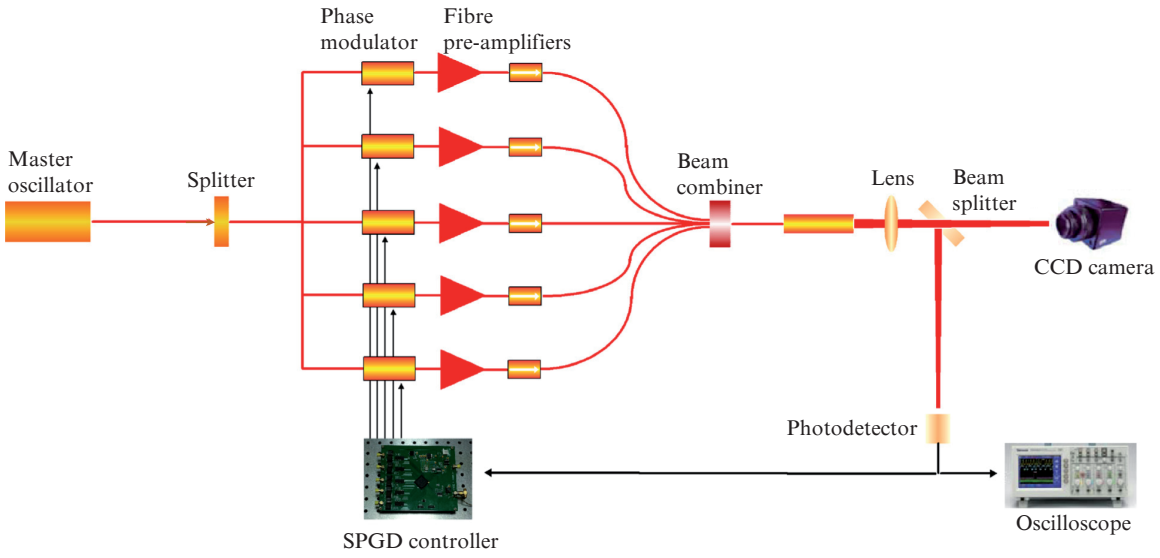

Figure 1. Scheme of the setup for coherent beam combining in a MOPA configuration using the SPGD algorithm.

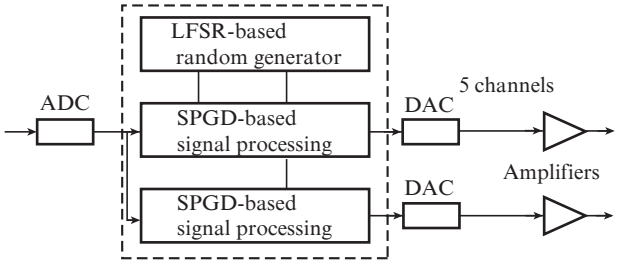

Figure 2. Block diagram of the phase controller based on the SPGD algorithm.

nite number of iterations (the iteration process can be terminated manually). Let the metric function $J = J(u)$ be specified, where $u = (u_1, u_2, \ldots, u_n)$ and u_j are the control signals applied to phase modulators. Each iteration of active phasing using this algorithm works as follows:

1. Generation of statistically independent random perturbations converted to the voltages $\delta u^{(k)} = \{\delta u_1, \delta u_2, \ldots, \delta u_n\}^{(k)}$ (k is the iteration number and n is the number of channels).

2. Application of control voltages with positive perturbations to the phase modulators and measurement of the metric function $J^+ = j(u + \delta u)$, and then measurement of the metric function $J^- = j(u - \delta u)$, corresponding to negative perturbations.

3. Calculation of the difference $\delta J = J^+ - J^-$ and formation of new control voltages $u_j^{(k+1)} = u_j^{(k)} - \xi \delta J^{(k)} \delta u_j^{(k)}$, where $\xi = \gamma_k / \sigma^2$, γ_k is the gain and k is the iteration step number.

3. Design of the phase controller

Figure 2 shows the block diagram of the phase controller designed. At each iteration, the FPGA, being the core of the controller, generates the random perturbation vector $\delta u^{(k)}$ so that the positive and negative perturbation signals $u^{(k)} \pm \delta u^{(k)}$ are applied to the phase modulators through the digital-to-analogue converters (DAC) and the voltage amplifiers, which make the phases of the laser beams change. Thus, the evaluation functions $J_+^{(k)}$ and $J_-^{(k)}$ detected in Fig. 1 are changed. Then, the evaluation functions are converted into digital signals from the analogue-to-digital converters (ADC). According to the gradient of the evaluation function and output, the FPGA replaces the control parameter. The above steps are repeated until the phase controllers are put off.

3.1. Control bandwidth

The characteristic time delays of the performance evaluation function is shown in Fig. 3. In the coherent combining system, the 0-dB bandwidth of the photodetector is 17 MHz, and its time delay is 59 ns. The time delay of the ADC (AD9224) is 13 ns. Thus, the time delay of the performance evaluation function is $t_1 = 72$ ns.

The output delay of the control signal is determined by the time delay between the moment of the output of the control signal in the algorithm control chip and the phase response time generated in the phase modulator. The output of the control signal from the FPGA is processed by the DAC (AD768) whose time delay is 10 ns and enters the amplifier

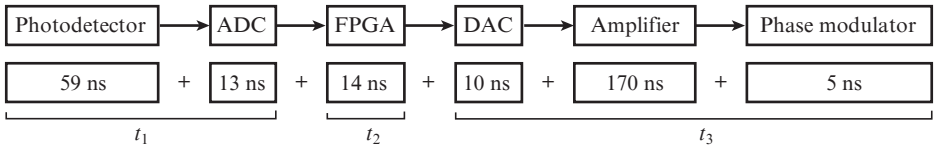

Figure 3. Time delays of the system control.

whose time delay is 170 ns. Then, it is applied to the phase modulator whose time delay is 5ns. The total delay is 185 ns.

The data processing delay of the algorithm controller (t_2 = 4 ns) is equal to the time delay between the moment of the input of the performance evaluation function and the control signal in the FPGA.

According to the above analysis, the single iteration time of the system is $T_0 = 2t_1 + t_2 + 2t_3$, which is 528 ns, and the iteration rate is 1.9 MHz, which is close to 2 MHz. After the optimisation of the parameters, the control bandwidth of the system for $M = 5$ beams is

$$F = (8MT_0)^{-1} = 50 \text{ kHz}. \quad (1)$$

Thus, the average compensation bandwidth of CBC for 2 or 20 channels is 125 kHz or 12.5 kHz, respectively.

3.2. Control accuracy

The control accuracy of the actual system can be evaluated in our case as

$$\delta\lambda = \frac{\delta u}{2V_\pi}\lambda = \frac{1}{21}\lambda, \quad (2)$$

where V_π is the modulator voltage changing the radiation phase by π.

4. Experiment on coherent beam combining with a phase controller

We have carried out an experiment on coherent combining of five fibre lasers using the phase controllers designed (see Fig. 1). Because the experiment is performed to verify the performance of the controller, fibre amplifiers are not added to the configuration.

According to theoretical calculations, in SPGD coherent combining experiment, the voltage perturbations should be subject to the Bernoulli distribution. The evaluation function J is defined as the energy detected by the detector. The control voltage has the form

$$u_j^{(k+1)} = u_j^{(k)} + \frac{\gamma_n}{\sigma^2}\frac{(J^+ - J^-)}{J_{\max}}\delta u_j^{(k)}. \quad (3)$$

In accordance with formula (3), the voltage signal u applied to the phase modulator is constantly iterated and updated. To find the perturbation amplitude σ and the gain γ, we used the following approach. Firstly, using a fixed perturbation amplitude of 0.3 rad s^{-1}, the gain was varied in the range from 0.28 to 0.8. At $\gamma = 0.28$ the evaluation function J rises slowly and requires many iterative steps for convergence. At $\gamma = 0.8$, the evaluation function J oscillates, and the control of the combining for five beams is unstable (Fig. 4).

At $\gamma = 0.5$ the algorithm is stable (Fig. 5) and J = 980 mV, which is 19.6 times for a single output. Thus, the combining efficiency reaches 78.4%.

To find the maximum of the evaluation function and to avoid falling into the local minima or oscillation, the improved control strategy utilising the variable gain (variable perturbation amplitude) is implemented in the experiment to obtain a higher combining efficiency. The gain in the SPGD algorithm is defined as:

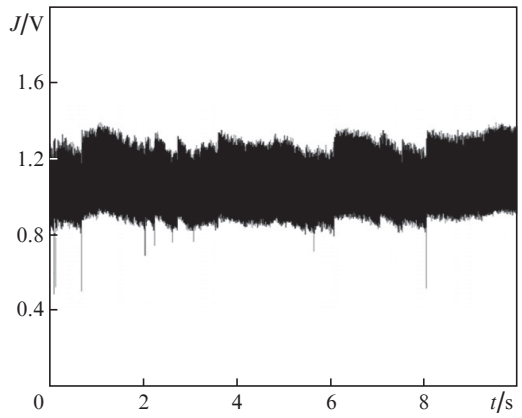

Figure 4. Evaluation function J for five beams at $\gamma = 0.8$.

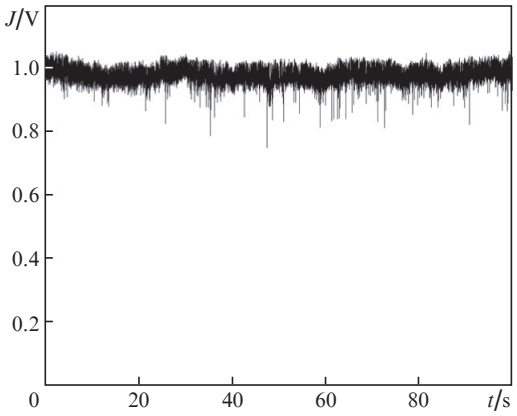

Figure 5. Evaluation function J for five beams at $\gamma = 0.5$.

$$\frac{\gamma}{\sigma^2}\frac{1}{J_{\max}} = \text{C} = \text{const}, \quad (4)$$

where $J_{\max}$ is the maximum value of the evaluation function in an open loop. The perturbation amplitude $u_r(\sigma)$ is divided into nine grades:

$$\begin{aligned}
&J > 95\%J_{\max},\ u_r = 0.111 \text{ rad};\\
&J > 90\%J_{\max},\ u_r = 0.111 \text{ rad};\\
&J > 85\%J_{\max},\ u_r = 0.147 \text{ rad};\\
&J > 80\%J_{\max},\ u_r = 0.184 \text{ rad};\\
&J > 75\%J_{\max},\ u_r = 0.221 \text{ rad};\\
&J > 70\%J_{\max},\ u_r = 0.258 \text{ rad};\\
&J > 65\%J_{\max},\ u_r = 0.295 \text{ rad};\\
&J > 60\%J_{\max},\ u_r = 0.332 \text{ rad};\\
&J > 60\%J_{\max},\ u_r = 0.405 \text{ rad}.
\end{aligned} \quad (5)$$

Figure 6 shows the change in J with changing the gain C in the oscilloscope display. If the gain is too large or too small, the phase locking will be unstable. In Fig. 6a (C = 0.00073),

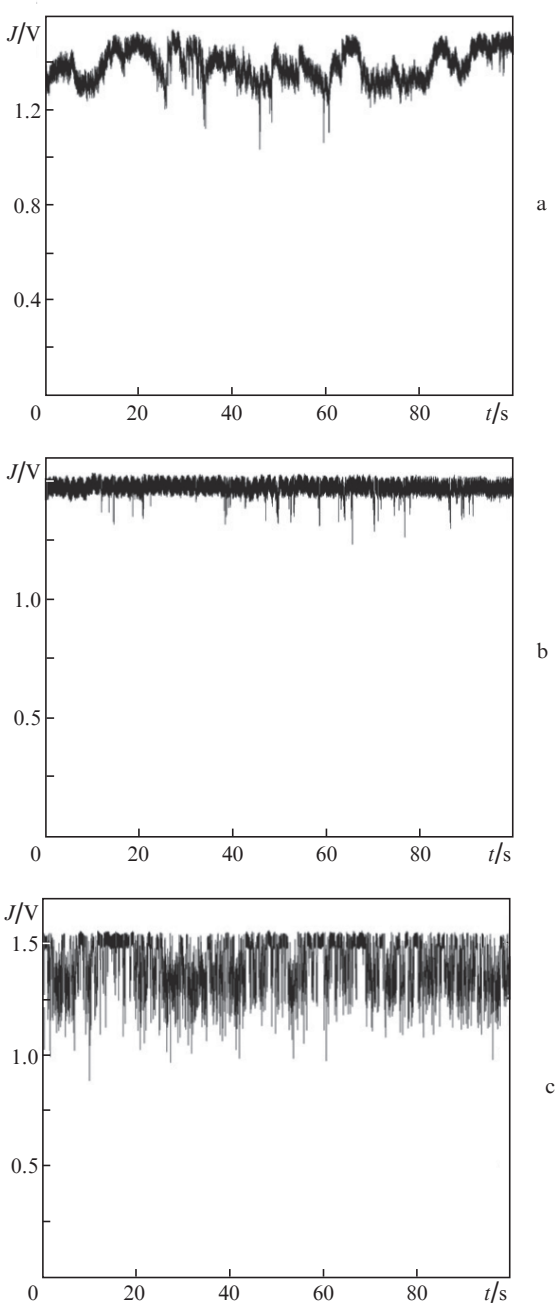

Figure 6. Evaluation function J at C = (a) 0.00073, (b) 0.00317 and (c) 0.03125.

the phase control is unstable and the signal power experiences large fluctuations. At an optimal C = 0.00317 (Fig. 6b), the phase control is stable, and at C = 0.03125, the phase control is unstable again.

When the phase controller does not execute the SPGD algorithm, the system is in the open-loop state and the value of J is constantly changed. When the system goes from the open-loop to the closed-loop state, the value of J becomes stable (Fig. 7). In the closed loop, the average value of the evaluation function increases by 23 times than that in the single output and the combining efficiency is 92% due to the improved control strategy with a variable gain.

The intensity distribution of the light spot in the far field also depends on the phase controller operation (Fig. 8): When the phase controller performs the SPGD algorithm, the power

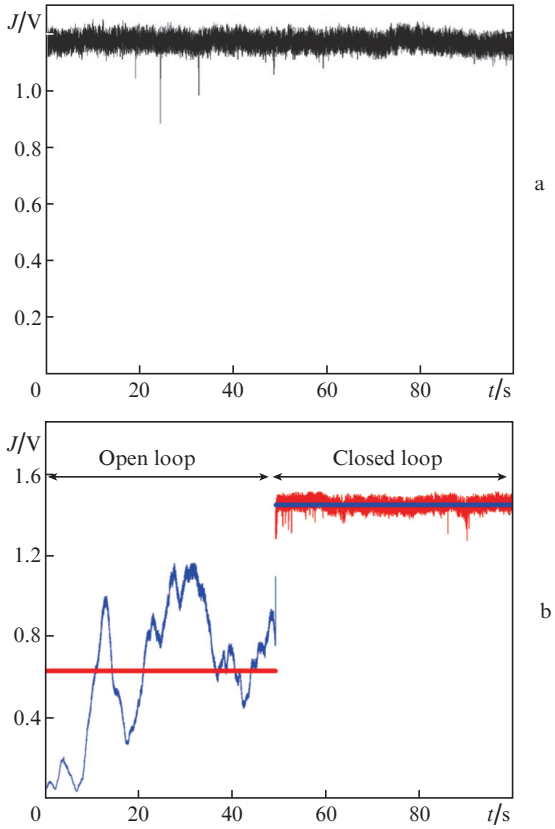

Figure 7. (a) Evaluation function J for five fibre lasers in the closed-loop state and (b) during the transition from the open-loop state into the closed-loop state.

of the output beam increases and the camera is always in saturation.

5. Conclusions

A phase controller for coherent beam combining of fibre lasers has been designed and manufactured based on the stochastic parallel gradient descent algorithm. Its iteration rate is more than 1.9 MHz and control accuracy is better than $\lambda/20$, which is significantly higher than that of similar previously designed controllers. The compensation bandwidth of the phase controller designed for 5 or 20 channels is 50 kHz or 12.5 kHz, respectively. In the experiment on the CBC for five fibre lasers, when use is made of the improved control strategy with a variable gain, the average value of the evaluation function increases by 23 times than that in the single output, and the combining efficiency is 92%.

Acknowledgements. This work is supported by the China Academy Engineering Physics Foundation (Grant No. 2009A0404024) and the Development Foundation of IFP (Grant No. SFZ20130302).

References

1. Agust S.J., Fan T.Y., Sanchez A. *Opt. Lett*., **29** (5), 474 (2004).
2. Hou J., Xiao R., Jiang Z.F. *Chin. Phys. Lett*., **22** (9), 2273 (2005).
3. Sevian A., Andrusyak O., Ciapurin I. *Opt. Lett*., **33** (4), 354 (2008).
4. Anderegg J., Brosnan S., Cheung E. *Proc. SPIE Int. Soc. Opt. Eng*., **6102**, 61020U-1 (2006).
5. Slavk R., Parmigiani F., Kakande J. *Nature Photon*., **4**, 690 (2010).

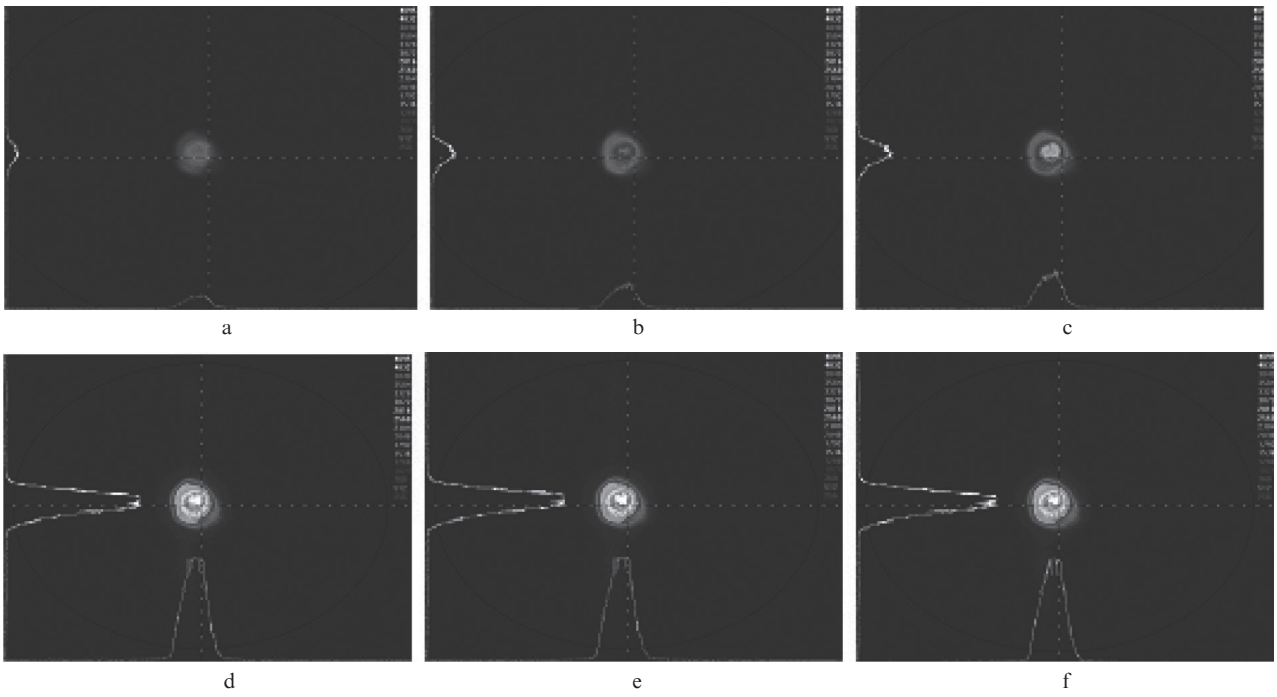

Figure 8. (a)–(c) Far-field intensity distribution when the system in the open-loop state and (d)–(f) during the transition from the open-loop state into the closed-loop state.

6. Kurita T., Sueda K., Tsubakimoto K. *Opt. Express*, **18** (14), 14541 (2010).
7. Huang Z.M., Zhang D.Y., Luo Y.Q., Li J.F., Liu C.L. *Appl. Phys. B*, **101** (3), 559 (2010).
8. Fan T.Y. *IEEE J. Sel. Top. Quantum Electron*., **11** (3), 567 (2005).
9. Huang Z.M., Liu C.L., Li J.F., Zhang D.Y., Wang H.F., Luo Y.Q., Hu Q.Q. *Laser. Phys*., **22** (8), 1347 (2012).
10. Xiao R., Hou J., Liu M. *Opt. Express*, **16** (3), 2015 (2008).
11. Shay T.M. *Opt. Express*, **14** (25), 12188 (2006).
12. Shay T.M., Benham V. *Proc. SPIE Int. Soc. Opt. Eng*., **5550**, 313 (2004).
13. Liu L., Vorontsov M.A. *Proc. SPIE Int. Soc. Opt. Eng*., **5895**, 58950P (2005).
14. Weyrauch T., Vorontsov M.A., Carhart G.W. O*pt. Lett*., **36** (22), 4455 (2011).
15. Ma Y., Zhou P., Wang X., Ma H., Xu X., Si L., Liu Z., Zhao Y. *Opt. Lett*., **35** (9), 1308 (2010).
16. Liu L., Vorontsov M.A., Polnau E.P. *Proc. SPIE Int. Soc. Opt. Eng*., **6708**, 67080K-1 (2007).
17. Vorontsov M.A., Weyrauch T., Beresnev L.A. *IEEE J. Sel. Top. Quantum Electron*., **15** (2), 269 (2009).
18. Yang R.F, Yang P., Shen F. *Acta Phys. Sinica*, **58** (12), 8287 (2009).
19. Wang X.L., Zhou P., Ma Y.X. *Acta Phys. Sinica*, **59** (2), 973 (2010).
20. Wang S.H., Liang Y.H., Ma H.T. *Chinese J. Lasers*, **36** (10), 2763 (2009).